Color Fourier-Mellin Descriptors for Image Recognition

José Mennesson, Christophe Saint-Jean, Laurent Mascarilla

Color Fourier-Mellin Descriptors for Image Recognition

J. Mennesson[a,*], C. Saint-Jean[b], L. Mascarilla[b]

[a] *Laboratory LIFL, Cité scientifique, Villeneuve d'Ascq, FRANCE*
[b] *Laboratory MIA, Avenue Michel Crépeau, La Rochelle, FRANCE*

Abstract

We propose new sets of Fourier-Mellin descriptors for color images. They are constructed using the Clifford Fourier Transform of Batard et al. (2010) and are an extension of the classical Fourier-Mellin descriptors for grayscale images. These are invariant under direct similarity transformations (translations, rotations, scale) and marginal treatment of colors images is avoided. An implementation of these features is given and the choice of the bivector (a distinguished color plane which parameterizes the Clifford Fourier Transform) is discussed. The proposed formalism extends and clarifies the notion of direction of analysis as introduced for the quaternionic Fourier-Mellin moments (Guo and Zhu, 2011). Thus, another set of descriptors invariant under this parameter is defined. Our proposals are tested with the purpose of object recognition on well-known color image databases. Their retrieval rates are favourably compared to standard feature descriptors.

Keywords: Object recognition, Image retrieval, Invariant color descriptors, Frequency methods, Clifford algebra

1. Introduction

In the literature, there are many recent advances in terms of image recognition. The recognition process depends highly on discriminative and invariant descriptors. Two main approaches can be used: global methods which concern features calculated on the entire image (Bornard et al., 1986; Zhang and Lu, 2002; Teague, 1980) and local methods based on feature extraction around of keypoints (e.g. SIFT (Lowe, 1999), GLOH (Mikolajczyk and Schmid, 2005), FAST (Rosten et al., 2010)).

Among global methods, one can cite moment-based descriptors (Flusser et al., 2009) such as Hu invariants (Hu, 1962), Legendre moments or Zernike moments (Zernike, 1934). Other approaches based on the computation of an histogram can be used (Chapelle et al., 1999). An alternative to these methods is to define descriptors in the frequency domain. For example, the family of Fourier descriptors (Zhang and Lu,

*Corresponding author: Tel.: +33-359632233;
Email addresses: jose.mennesson@univ-lille1.fr (J. Mennesson), christophe.saint-jean@univ-lr.fr (C. Saint-Jean), laurent.mascarilla@univ-lr.fr (L. Mascarilla)

2002; Smach et al., 2008) is widely used because of their properties of invariance, speed of convergence, low computational time. Originally, the 1-D Fourier descriptors (Cosgriff, 1960; Arbter et al., 1990) are obtained through Fourier transform (FT) on a shape signature function derived from shape boundary coordinates. More recently, 2-D Fourier descriptors have been proposed. In this case, it is assumed that images contain only one object and that the background is uniform. The most common are the Generalized Fourier Descriptors (GFD) (Smach et al., 2008) (invariant under translation and rotation) and the Fourier-Mellin descriptors (Sheng and Arsenault, 1986; Derrode and Ghorbel, 2001) (invariant under translation, rotation and scale) computed from the Fourier-Mellin transform of a grayscale image. This later is widely applied in the field of document processing (Sheng and Arsenault, 1986; Grace and Spann, 1991).

Originally, the Fourier-Mellin method is based on the polar transformation of the image, followed by a Fourier transform then a Mellin transform. More recently, Derrode and Ghorbel (2001) proposed a complete set of Fourier-Mellin descriptors using an analytical Fourier-Mellin transform. Three algorithms which consider the original image, its polar and log-polar forms are defined to accelerate the computation of these descriptors. This work emphasized the effect of the polar and log-polar transformation of an image which are not exact (numerical interpolation is needed). This is a well-known open issue that is currently under investigation by Fenn et al. (2007) and Liu et al. (2006).

Extending these approaches to color images is not straightforward because they rely on the definition of a Fourier transform on color images. More precisely, these images are no longer viewed as functions from $\mathbb{R}^2$ to $\mathbb{R}$ but from $\mathbb{R}^2$ to $\mathbb{R}^3$: the value of each pixel is not a scalar but a vector. A classical generalization to color images is the use of an *ad hoc* approach like the marginal one (Smach et al., 2008), *i.e.* a separate treatment of each red, green, blue color plane. Another method consists in encoding *RGB* color space within the space of pure quaternions. In this framework, Sangwine and Ell proposed a Quaternionic Fourier Transform (QFT) (Sangwine and Ell, 2000). This one is defined by replacing the imaginary unit i in the exponential of the Fourier transform by a pure unit quaternion μ, interpreted as a direction of analysis. This latter is commonly set as the gray level axis to obtain a luminance/chrominance analysis. Based on this QFT, Guo and Zhu (2011) derivated a quaternionic extension of the Fourier-Mellin moments (Sheng and Arsenault, 1986) with application to color image registration.

Clifford algebras (Hestenes and Sobczyk, 1987), which contains the quaternion algebras, can also be used to embed and process color images. In our previous works, the GFD have been extended in several ways to color images yielding the Generalized Color Fourier Descriptors (Mennesson et al., 2010) ($GCFD1$ and $GCFD2$) by using a Clifford Fourier transform (CFT) dedicated to color images (Batard et al., 2010).

In this paper, we define new sets of Fourier-Mellin descriptors for color images, namely *poFMD*, *CFMD* and *CFMDi*, which are different extensions of the Fourier-Mellin moments computed from the *CFT*.
In section 2, definition and a fast implementation of the *CFT* are recalled. Then, in section 3, 4 and 5, the three differents color Fourier-Mellin descriptors are defined (their invariance under translations, rotations and scale changes are proven in Appendix A and Appendix B). Finally, in section 6 our proposals are tested with the purpose of

object recognition and retrieval on well-known color image databases. Their retrieval rates are compared to standard feature descriptors.

2. Clifford Fourier Transform For Color Images (*CFT*)

Classical Fourier transforms (Bracewell, 1986; Bornard et al., 1986; Ghorbel, 1993) are usually defined for complex valued functions that suited well for gray level, and not for color images. The most immediate solution is to compute three Fourier transforms independently on each channel of the color image. This marginal method raises problems as emergence of false colors in the case of color image filtering.

To avoid this marginal treatment, Batard et al. (2010) defined a Fourier transform for $L^2(\mathbb{R}^2;\mathbb{R}^4)$ functions using Clifford Algebras (Hestenes and Sobczyk, 1987). This one is different from other color Fourier transforms (Sangwine and Ell, 2000; Ell, 1992) because it clarifies relations between the Fourier transform and the action of the translation group through a spinor group. This point of view justifies the necessity of choosing a direction of analysis. It is also demonstrated in (Batard et al., 2010) that the quaternionic Fourier transform defined by Sangwine and Ell (2000) is a particular case of this definition.

2.1. Definition of the CFT

The *RGB* pixels of a color image can be embedded in $\mathbb{R}^1_{4,0}$ algebra (vectors of $\mathbb{R}_{4,0}$) as follows

$$f(\mathbf{x}) = r(\mathbf{x})\mathbf{e_1} + g(\mathbf{x})\mathbf{e_2} + b(\mathbf{x})\mathbf{e_3} + 0\ \mathbf{e_4}. \tag{1}$$

with $\mathbf{x} = (x_1, x_2)$ and r, g, b are red, green and blue channels of a color image.

The color Clifford Fourier Transform *CFT* (Batard et al., 2010) of $f \in L^2(\mathbb{R}^2;\mathbb{R}^1_{4,0})$ functions (*i.e.* a color image) with respect to an unit bivector B (identifiable to an analysis plane) is the vector-valued function

$$\widehat{f_B}(\mathbf{u}) = \int_{\mathbb{R}^2} e^{\frac{1}{2}\langle \mathbf{u},\mathbf{x}\rangle B} e^{\frac{1}{2}\langle \mathbf{u},\mathbf{x}\rangle I_4 B} f(\mathbf{x}) e^{-\frac{1}{2}\langle \mathbf{u},\mathbf{x}\rangle I_4 B} e^{-\frac{1}{2}\langle \mathbf{u},\mathbf{x}\rangle B} d\mathbf{x} \tag{2}$$

where I_4 is the pseudo-scalar of $\mathbb{R}_{4,0}$ and $I_4 B$ is an unit bivector which is orthogonal to B. This color Fourier transform is invertible and the inverse of the *CFT* is given by

$$f(\mathbf{x}) = \int_{\mathbb{R}^2} e^{-\frac{1}{2}\langle \mathbf{u},\mathbf{x}\rangle B} e^{-\frac{1}{2}\langle \mathbf{u},\mathbf{x}\rangle I_4 B} \widehat{f_B}(\mathbf{u}) e^{\frac{1}{2}\langle \mathbf{u},\mathbf{x}\rangle I_4 B} e^{\frac{1}{2}\langle \mathbf{u},\mathbf{x}\rangle B} d\mathbf{u} \tag{3}$$

A vector can be decomposed in a parallel part and an orthogonal part depending on the choice of the bivector B (Hestenes and Sobczyk, 1987). Being f an image and B a bivector, this decomposition is $f = fBB^{-1} = (f \cdot B + f \wedge B)B^{-1} = f_{\|B} + f_{\perp B}$ where $f_{\|B} = (f \cdot B)B^{-1}$ (resp. $f_{\perp B} = (f \wedge B)B^{-1}$) is the parallel (resp. orthogonal) projection of f on a bivector B.

After some elementary calculations, Eq. 2 can be rewritten depending on this decomposition $\widehat{f_B}(\mathbf{u}) = \widehat{f_{\|B}}(\mathbf{u}) + \widehat{f_{\perp B}}(\mathbf{u})$ where

$$\widehat{f_{\|B}}(\mathbf{u}) = \int_{\mathbb{R}^2} e^{\frac{\langle \mathbf{u},\mathbf{x}\rangle}{2} B} f_{\|B}(\mathbf{x}) e^{-\frac{\langle \mathbf{u},\mathbf{x}\rangle}{2} B} d\mathbf{x} = \int_{\mathbb{R}^2} f_{\|B}(\mathbf{x})\ e^{-\langle \mathbf{u},\mathbf{x}\rangle B} d\mathbf{x} \tag{4}$$

$$\widehat{f_{\perp B}}(\mathbf{u}) = \int_{\mathbb{R}^2} f_{\perp B}(\mathbf{x})\, e^{-\langle \mathbf{u},\mathbf{x}\rangle I_4 B} d\mathbf{x} \tag{5}$$

Now, the bivectors B and I_4B can be identified to a pure imaginary number i since $B^2 = (I_4B)^2 = -1$. Equations 4 and 5 can be calculated using two usual fast Fourier transforms.

Depending on the application, it may be advisable to reconstruct $\widehat{f_B}$ from $\widehat{f_{\parallel B}}$ and $\widehat{f_{\perp B}}$. The problem can be modelled as a system of four equations where the unknowns are the coordinates of $\widehat{f_B}$ in the basis $\{\mathbf{e_1}, \mathbf{e_2}, \mathbf{e_3}, \mathbf{e_4}\}$ (see details in (Mennesson et al., 2011, 2012)).

Computational complexity of the color Clifford Fourier transform, including the reconstruction step, is $O(n\ log(n))$ where n is the number of pixels of the considered image. Indeed, this one requires only eight projections ($O(n)$) and two fast Fourier transforms ($O(n\ log(n))$).

The bivector B is a required parameter of the *CFT*, hence of any derivated descriptors that are not invariant to the parameter. The choice of a given B can be left to the user, assuming some prerequired knowledge about the dataset at hand. The next subsection gives some guidelines for such choice.

2.2. Practical construction of a bivector B

An unit bivector B can be obtained with taking the geometric product of two unit vectors $\mathbf{v_1}$, $\mathbf{v_2}$, orthogonal to each other w.r.t. the quadratic form Q. The corresponding bivector can be geometrically interpretable as the oriented plane spanned by $\mathbf{v_1}$ and $\mathbf{v_2}$. Note that when $\mathbf{v_1}$ and $\mathbf{v_2}$ are not colinear, it is always possible to find an Q-orthonormal basis taking the rejection of $\mathbf{v_2}$ on $\mathbf{v_1}$ and scaling to unity. If the bivector $B_{\mathbf{c}} = \mathbf{c} \wedge \mathbf{e_4}$ (with $\mathbf{c} = c_1\mathbf{e_1} + c_2\mathbf{e_2} + c_3\mathbf{e_3}$ a normed color vector chosen by the user) is considered, the direction of analysis of the *CFT* is the same as the *QFT* by considering the unit quaternion $\mu = c_1 i + c_2 j + c_3 k$ in (Ell and Sangwine, 2007). Let's recall that the *QFT* is used by Guo and Zhu (2011) with $\mu = \frac{i+k}{\sqrt{2}}$.

In contrast of the quaternionic Fourier transform, the bivector used in the *CFT* is more general and allows, for example, to take hue planes by taking bivectors of the form $B_{\underline{\mathbf{c}}} = \mathbf{c} \wedge \mathbf{gray} = \left(c_1\mathbf{e_1} + c_2\mathbf{e_2} + c_3\mathbf{e_3} \wedge \frac{\mathbf{e_1}+\mathbf{e_2}+\mathbf{e_3}}{\sqrt{3}}\right)$ with $\mathbf{c}$ a color. In this case, the two vectors must be orthogonalized using the following rejection formula :

$$\mathbf{v_3} = (\mathbf{v_2} \wedge \mathbf{v_1})\mathbf{v_1}^{-1} \tag{6}$$

with $\mathbf{v_1}$, $\mathbf{v_2}$ two non orthogonal vectors, $\mathbf{v_3}$ a vector orthogonal to $\mathbf{v_1}$ in the plane generated by $\mathbf{v_1} \wedge \mathbf{v_2}$ and $\wedge$ the outer product.

In section 6, the sensitivity to the choice of B is tested and is emphasized by different applications.

3. The parallel-orthogonal Fourier-Mellin Descriptors (*poFMD*)

In this section, we propose to compute the classical Fourier-Mellin moments (FMM) on parallel and orthogonal parts of the *CFT* as in (Mennesson et al., 2011) with the

Generalized Fourier Descriptors. The two sets of moments can be concatenated and normalized to obtain a description vector.

3.1. Definition of the poFMM

Definition 1. *The Fourier-Mellin Moments (*FMM*) are defined for an image $f \in L^2(\mathbb{R}^2, \mathbb{C})$, expressed in polar coordinates, as*

$$FMM_f(m,n) = \int_{r=0}^{\infty} \int_{\theta=0}^{2\pi} r^{m-1} f(r,\theta) e^{-in\theta} d\theta dr \tag{7}$$

The poFMM *descriptors are the concatenation of the* FMM *computed on parallel and orthogonal parts of the color image with respect to a bivector B,* i.e.

$$poFMM_{f,B}(m,n) = \left\{ FMM_{f_{\parallel B}}(m,n), FMM_{f_{\perp B}}(m,n) \right\} \tag{8}$$

The set of descriptors is not yet invariant under translation, rotation and scale. A normalization step must be applied to obtain these invariances (Sheng and Arsenault, 1986).

3.2. Computation of the poFMD

The *poFMD* are obtained by taking the magnitude of the *poFMM* and by dividing by the first coefficient of each row, *i.e.* $poFMM_{f,B}(m,0)$. The first manipulation provides rotation invariance and, the second, scale invariance (see (Sheng and Arsenault, 1986)).

Definition 2. *The* poFMD *are contained in a $\mathbb{R}^{M \times N}$ vector and are defined for a color image $f \in L^2(\mathbb{R}^2, \mathbb{R}^1_{4,0})$, expressed in polar coordinates, as*

$$\begin{aligned} poFMD_{f,B} \quad = \quad & \left\{ \frac{|poFMM_{f,B}(1,1)|}{|poFMM_{f,B}(1,0)|}, \frac{|poFMM_{f,B}(1,2)|}{|poFMM_{f,B}(1,0)|}, \ldots, \right. \\ & \left. \frac{|poFMM_{f,B}(m,n)|}{|poFMM_{f,B}(m,0)|}, \ldots, \frac{|poFMM_{f,B}(M,N)|}{|poFMM_{f,B}(M,0)|} \right\} \end{aligned}$$

where $M \times N$ is the number of considered moments and $|\,|$ the modulus of a complex.

It is obvious that these descriptors depends on B, which parameterizes the parallel-orthogonal decomposition of the color image.

4. The Color Fourier-Mellin Descriptors(*CFMD*)

In this section, the Color Fourier-Mellin Moments (*CFMM*) are defined using the *CFT* instead of the classical Fourier transform. It follows the approach of Guo and Zhu (2011) for the quaternionic Fourier transform. Just like for the *poFMM*, these moments are normalized to obtain invariant descriptors.

4.1. Definition

Definition 3. *The Color Fourier-Mellin Moments (*CFMM*) are defined for a color image $f \in L^2(\mathbb{R}^2, \mathbb{R}^1_{4,0})$, expressed in polar coordinates, as*

$$CFMM_{f,B}(m,n) = \int_{r=0}^{\infty} \int_{\theta=0}^{2\pi} r^{m-1} e^{\frac{n\theta}{2}(B+I_4B)} f(r,\theta) e^{-\frac{n\theta}{2}(B+I_4B)} d\theta dr \tag{9}$$

with B a unit bivector.

The properties of the *CFMM* are analyzed in Appendix A.

4.2. Computation of the CFMD

The Color Fourier-Mellin Descriptors (*CFMD*) are obtained by taking the magnitude of the *CFMM* and by dividing by the first coefficient of each row, *i.e.* $CFMM_{f,B}(m,0)$. The first manipulation provides rotation invariance and the second, scale invariance (see theorem 1 and 2 in Appendix A). The results for empirical invariance to these geometrical transformations and for sensitivity to the choice of B are provided in Appendix C.

Definition 4. *The Color Fourier-Mellin Descriptors (*CFMD*) are contained in a $\mathbb{R}^{M\times N}$ vector and are defined for a color image $f \in L^2(\mathbb{R}^2, \mathbb{R}^1_{4,0})$, expressed in polar coordinates, as*

$$\begin{aligned} CFMD_{f,B} \quad = \quad & \left\{ \frac{|CFMM_{f,B}(1,1)|}{|CFMM_{f,B}(1,0)|}, \frac{|CFMM_{f,B}(1,2)|}{|CFMM_{f,B}(1,0)|}, \ldots, \right. \\ & \left. \frac{|CFMM_{f,B}(m,n)|}{|CFMM_{f,B}(m,0)|}, \ldots, \frac{|CFMM_{f,B}(M,N)|}{|CFMM_{f,B}(M,0)|} \right\} \end{aligned}$$

where $M \times N$ is the number of considered moments and $|\,|$ the magnitude of a vector.

With the normalization of the moments, it is obvious that an invariance under global luminance changes is also achieved.

4.3. Invariance under translation

The *CFMD* are invariant under rotations and scale by construction, but not by translation. To solve this problem, the center of the image must be estimated to define the origin of coordinates. This can be done using a direct extension of the image moments for color images as in (Guo and Zhu, 2011).

Definition 5. *Being a color image $f \in L^2(\mathbb{R}^2, \mathbb{R}^1_{4,0})$, the color image moments are defined as follows :*

$$M^c_{p,q} = \int_{-\infty}^{+\infty} \int_{-\infty}^{+\infty} x_1^p x_2^q |f(x_1,x_2)| dx_1 dx_2 \tag{10}$$

where $|\,|$ is the magnitude of a vector.

The center of the image is determined by $\overline{x_1} = M^c_{1,0}/M^c_{0,0}$ and $\overline{x_2} = M^c_{0,1}/M^c_{0,0}$. It can be easily proved that if the color image is translated by $(\Delta_{x_1}, \Delta_{x_2})$, *i.e.* $f(x_1', x_2') = f(x_1 + \Delta_{x_1}, x_2 + \Delta_{x_2})$ then $f(x_1' - \overline{x_1'}, x_2' - \overline{x_2'}) = f(x_1 - \overline{x_1}, x_2 - \overline{x_2})$. So, if the origin of coordinates is translated to the color image centroid, the invariants computed on the resulting image are invariant under translation.

4.4. Implementation of the CFMD

To be able to compute the *CFMD*, one has to compute the *CFMM* using the fast implementation of the Clifford Fourier Transform given in section 2. Eq. 9 can be rewritten as follows.

Let f a color image of size $n_1 \times n_2$, the discrete implementation of the *CFMM* is given by

$$CFMM_{f,B}(m,n) = \sum_{r=0}^{r_{max}} \sum_{\theta=0}^{2\pi} r^{m-1} e^{\frac{n\theta}{2}(B+I_4B)} f(r,\theta) e^{-\frac{n\theta}{2}(B+I_4B)} \Delta\theta \Delta r \tag{11}$$

$$= \sum_{r=0}^{r_{max}} r^{m-1} \left(\sum_{\theta=0}^{2\pi} e^{\frac{n\theta}{2}(B+I_4B)} f(r,\theta) e^{-\frac{n\theta}{2}(B+I_4B)} \Delta\theta \right) \Delta r \tag{12}$$

with $r_{max} = max\{\sqrt{(x_1 - \overline{x_1}) + (x_2 - \overline{x_2})} | x_1 = 1, 2, ..., n_1; x_2 = 1, 2, ..., n_2\}$, $\Delta r = r_{max}/(nr - 1)$, $\Delta\theta = (2\pi)/na$, nr and na are respectively the number of radius and angle values in polar coordinates.

The *CFMM* computation can be interpreted as the computation of one-dimensional *CFT* with respect to variable θ, followed by the discrete summation in Eq. 12.

The computational complexity of the *CFMM* is $O(M\ N\ log(N))$ where N is the number of angles considered (*i.e.* the maximum number of columns) of the polar image and M the maximum of radial frequencies to compute.

5. Color Fourier-Mellin Descriptors Invariant under the Choice of B (*CFMDi*)

Although our method is translation, rotation and scale invariant, it still depends on the choice of a bivector. Depending on the application at hand, invariance with respect to this parameter may be required. Indeed, if a privileged color is available (dominant color of objects of interest, background color and so on), the previous *CFMM* are perfectly well suited. But, when no such knowledge is available an alternative, bivector invariant, descriptor may be required.

Definition 6. *The definition of the Color Fourier-Mellin Moment invariant under the choice of the bivector(*CFMMi*) for a color image $f \in L^2(\mathbb{R}^2, \mathbb{R}^1_{4,0})$ in polar coordinates, is*

$$CFMMi_{f,B}(m,n) = \int_{r=0}^{\infty} r^{m-1} \left(\left| \int_{\theta=0}^{2\pi} e^{\frac{n\theta}{2}(B+I_4B)} f(r,\theta) e^{-\frac{n\theta}{2}(B+I_4B)} d\theta \right|^2 + \right.$$

$$\left. \left| \int_{\theta=0}^{2\pi} e^{-\frac{n\theta}{2}(B+I_4B)} f(r,\theta) e^{\frac{n\theta}{2}(B+I_4B)} d\theta \right|^2 \right) dr \tag{13}$$

$$= \int_{r=0}^{\infty} r^{m-1} \left(\left| \widehat{f_B}(m,n) \right|^2 + \left| \widehat{f_B}(m,-n) \right|^2 \right) dr \tag{14}$$

with B a unit bivector.

The properties of the *CFMMi* are provided in Appendix B. The *CFMMi* must be normalized in the same way as the *CFMM* to achieve the invariance under rotation and scale. This is done by the following definition.

Definition 7. *The Color Fourier-Mellin Descriptors invariant under the choice of the bivector (*CFMDi*) are defined for a color image $f \in L^2(\mathbb{R}^2, \mathbb{R}^1_{4,0})$, expressed in polar coordinates, as*

$$CFMDi_f = \left\{ \frac{CFMMi_{f,B}(1,1)}{CFMMi_{f,B}(1,0)}, \frac{CFMMi_{f,B}(1,2)}{CFMMi_{f,B}(1,0)}, \ldots, \frac{CFMMi_{f,B}(m,n)}{CFMMi_{f,B}(m,0)}, \ldots, \frac{CFMMi_{f,B}(M,N)}{CFMMi_{f,B}(M,0)} \right\}$$

where $M \times N$ is the number of considered moments.

It must be emphasized that this invariance under the choice of the bivector is not an invariance to the colors present in the image. This is just a way to obtain color Fourier-Mellin descriptors without reference to some bivector B,*i.e.* no privileged direction of analysis. The results for empirical invariance to rotation and scale are provided in Appendix C.

6. Experiments

In this section, the *poFMD*, *CFMD*, *CFMDi* are evaluated and compared in the context of color image recognition and image retrieval. The choice of the bivector is discussed and proposals are compared to classical Fourier-Mellin Moments *FMM* (Sheng and Arsenault, 1986) (128 desc.), classical Fourier-Mellin Moments computed on color channels R, G, B separately (FMM_{rgb}) (128 desc.), Generalized Color Fourier Descriptors *GCFD1* (Mennesson et al., 2010) (128 desc.), Zernike moments (Zernike, 1934) (72 desc.), original Local Binary Patterns (Ahonen et al., 2006) (256 desc.).

In these experimentations, it is assumed that there is just one object per image and that the background is uniform. Thus, we have decided not to compare our proposals with local methods for image recognition since they obey generally to very different rules. In particular for local methods, a huge set of descriptors is extracted from many keypoints and is combined in order to cope with occlusions and cluttered background. In this context, it becomes risky to guess whether the individual quality of the descriptors derived from their definition, their size or from the classifier used. By the way, some recent works (Andrade et al., 2012) showed that global and local descriptors may be combined successfully to improve the process of image recognition.

6.1. Image recognition experiments

To evaluate our descriptors different standard color image databases have been used. The choice of the bivector B, the parameter of the color Clifford Fourier transform, and the respective performances of the various descriptors in terms of recognition rates are discussed. In the following, the experimental protocol to test our approach is described.

6.1.1. Image databases

The databases used in this section are a modified version of COIL-100 and color FERET.

- To check rotation and scale invariance, **a modified version of COIL-100 (Nene et al., 1996) (Columbia Object Image Library) database** is used. Each image for this database (except the first of each class) is randomly rotated by an angle $\phi = [0, 360]$ and scaled by a factor $k \in [0.5, 1]$.
- The **color FERET database** (Phillips et al., 1998) is composed of face images of 1408 different persons, taken from different angles of view. In our tests, a set of 2992 images containing 272 persons equally represented by 11 pictures is selected and size of images is reduced to 128×128.

6.1.2. Descriptors extraction

In order to make a fair comparison, the length of each set is limited to 128, whatever the considered associated descriptors (*GCFD1*(Mennesson et al., 2012), *FMM*, FMM_{rgb}, *CFMD*, *CFMDi* or *poFMD*). The 128 *poFMD*(m,n) descriptors correspond to $m = 1, ..., 8$ and $n = 1, ..., 8$, the 128 $CFMD(m, n)$ descriptors and the *CFMDi*(m,n) descriptors correspond to $n = 1, ..., 11$ and $m = 1, ..., 12$ (the four last descriptors are removed).

6.1.3. Classification step

The classification step is performed using a standard Support Vector Machine SVM (Vapnik, 1998) using $LIBSVM$ implementation (Chang and Lin, 2001). Each descriptors set is used as feature vector in the classifier.

In our tests on the Modified COIL-100 and color FERET databases, the standard radial basis kernel (Gaussian kernel) is used in order to compare our results with those obtained in (Mennesson et al., 2010). Parameters σ (of the gaussian kernel) and C (the penalty coefficient) are set empirically by a 10-cross validation and a grid search (Duda et al., 2001) to maximize the recognition rate for each experiment (Chang and Lin, 2001). Other less sophisticated algorithm as *LDA* or *1-NN* (Jain et al., 1999) are also used to test the influence of the *SVM* on recognition rates obtained with our descriptors.

6.1.4. Experiment on modified COIL-100 *database*

In Fig. 1, the *poFMD* with the best bivector give better results than the other descriptors regardless of the method of classification. But, it seems to be much more dependent on the choice of the bivector than the other methods. Note that the differences between recognition rates obtained by the various descriptors with the *SVM* are not significant.

Concerning the *CFMDi*, the recognition rates obtained are better than the *CFMD* (except for the *LDA*) and the invariance of these descriptors under the choice of the bivector is verified. The FMM_{rgb} give a good recognition rate with the *LDA* and give results very close to *CFMDi* with other classifiers.

Concerning other global descriptors, one can note that the *GCFD1* and the *LBP* give worse results than those of the *CFMD*, *CFMDi* and *poFMD*. This is due to their non-invariance to scale changes. Moreover, the *GCFD1* are very sensitive to the choice of the bivector.

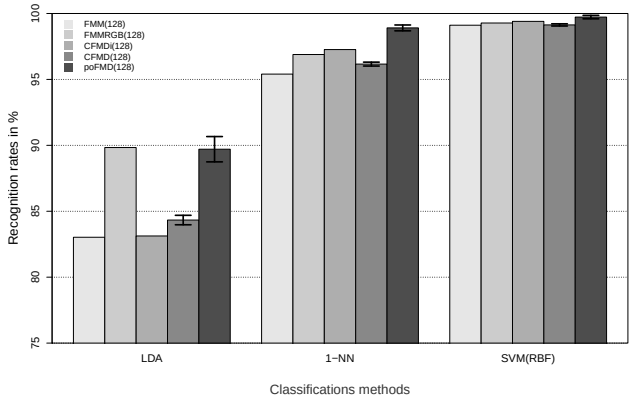

Modified COIL-100	ZM (72)	LBP (256)	GCFD1[1] (128)	poFMD[1] (128)
Reco. rates (SVM RBF)	83, 15%	40, 31%	86.34%	99.72%
Std in %	-	-	±3.51%	±0.13%

Figure 1: Modified COIL 100: Performance of *CFMD*, *CFMDi*, *poFMD* and *GCFD1* for 100 random bivectors (mean and standard deviation) and *FMM*, FMM_{rgb}, *ZM*, *LBP*

6.1.5. Experiment on color FERET database

Concerning the color FERET database (see Fig. 2), the recognition rates are lower because the background of images is not uniform. According to the experimentations conducted previously (Mennesson et al., 2010) with Clifford Fourier descriptors, we can suppose that the reconstructed $\widehat{f_B}$ carries less interesting frequency information when both $\widehat{f_{\|B}}$ and $\widehat{f_{\perp B}}$ are mutually discriminant (e.g. image contains high frequency in red and low frequency in blue). That is why it is not surprising that the *poFMD* and *GCFD1*, which are computed on the parallel and the orthogonal parts give the best results on this database. Compared with the *CFMD*, the standard deviation of the recognition rates obtained with these descriptors are high, showing their sensitivity to the choice of the bivector. Again, the FMM_{rgb} give better results than the other descriptors with the *LDA* classifier. However, they are less successful with other classifiers. For the *CFMDi*, the recognition rates are close to those obtained by the *CFMD* with the *1-NN* and the *SVM* and really better with a linear classifier *LDA*.

6.1.6. Application in image retrieval

This application aims at showing the efficiency of the Fourier-Mellin moments in a context of image retrieval, *i.e.* a query image is given by the user and the nearest

[1] for 100 random bivectors

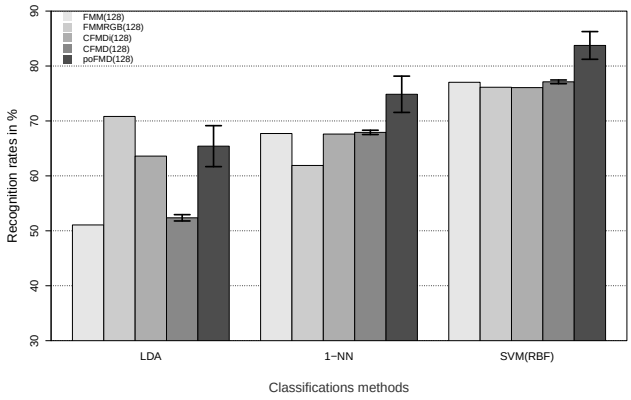

color FERET	ZM (72)	LBP (256)	GCFD1[1] (128)	poFMD[1](128)
Reco.rates (SVM RBF)	73, 66%	70, 79%	87, 41%	83, 74%
Std in %	-	-	±2, 78%	±2, 52%

Figure 2: color FERET: Performance of *CFMD*, *CFMDi*, *poFMD* and *GCFD1* for 100 random bivectors (mean and standard deviation) and *FMM*, FMM_{rgb}, *ZM*, *LBP*

images (using Euclidean distance) are returned. The modified COIL 100 database is used. The results are shown for 128 *poFMD*, *CFMDi*, *CFMD*, FMM_{rgb}, *FMM*, and *GCFD1*.

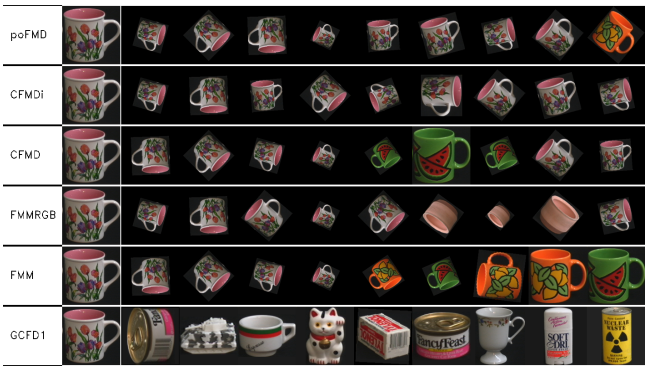

Figure 3: Modified COIL 100: nine best retrievals (ordered from left to right) for the query of the "colorful mug" (left column) with poFMD, CFMD, GCFD1 (parametrized by the bivector $B_{\mathbf{red}}$), CFMDi, FMM_{rgb} and FMM.

First experiment aims at retrieving a "colorful mug" (*cf.* Fig. 3, firsts column) in the database. Visual inspection (on shape and color) of the rows containing the retrieved objects, ordered according to the increasing distance to the query object, clearly shows that the best results are obtained with the *CFMDi* and the *poFMD* using the bivector

$B_{\mathbf{red}}$ with a score of $10/10$ and $9/10$. These descriptors take into account the color of the flower on the cup. The $CFMD$ fail 3 times but they succeed to recognize 3 other mugs, this is to be compared to FMM_{rgb} which retrieves mugs of different shapes but same dominant color. The classical *FMM* retrieve only 4 mugs but has difficulties to separate mugs of different colors. The *GCFD1* gives a poor score of $0/10$ due to its non-invariance under scale changes.

To confirm these observations, a second set of experiment where each of the 7200 images have been taken as request image has been made. The corresponding retrieval rate in terms of retrieval position is showed in Fig. 4.

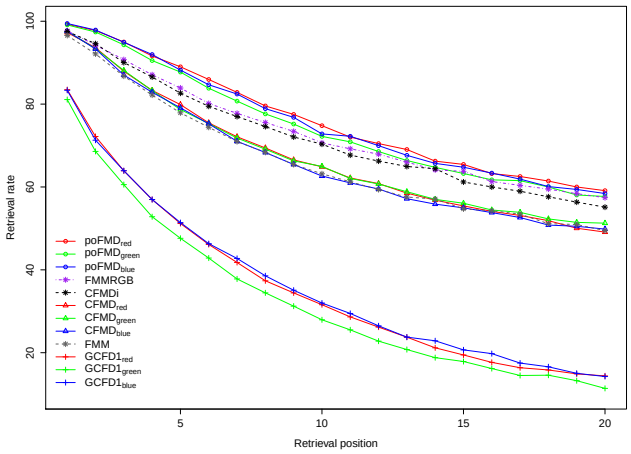

Figure 4: Modified COIL 100 : Retrieval rate of *poFMD*, *CFMD*, *CFMDi*, *FMM*, FMM_{rgb} and *GCFD1* for the 20 first retrieval positions

It is clear that the *poFMD* give better results than the other descriptors in terms of retrieval rate. The retrieval rates of the *CFMDi* and the FMM_{rgb} stay between retrieval rates curve of the *poFMD* and the *CFMD* one. Retrieval rates of the *FMM* seem to be slightly below the *CFMD*. Indeed, a good choice of bivector for one image can be a bad choice for an other. In this experiment, the results are averaged on all images, minimizing the influence of the choice of the bivector. Finally, one can see that the *GCFD1* give bad retrieval rates. This result is not surprising because, as in the Fig. 3, these descriptors are not invariant under scale changes. To summarize these experimentations, we can note again that the performance of the various descriptors can be ordered as $poFMD > FMM_{rgb} \simeq CFMDi > CFMD$. The computational time of these descriptors for one image (in milliseconds) with our implementation and a desktop computer (Intel core 2 processor 2.66 GHz $\times$ 2, 64-bit operating system, 2 Gbytes RAM) are reported in Table 1.

Table 1: Computation time of 128 poFMD, CFMD, CFMDi, FMM_{rgb} for one image of size 128×128

	FMM_{rgb}	poFMD	CFMD	CFMDi
Comp. time in ms.	4, 6 ms.	7, 4 ms.	10, 8 ms.	18, 5 ms.

7. Conclusion

In this article, the *poFMD* are first defined from the parallel and the orthogonal part of the Clifford Fourier transform. Then, the Quaternionic Fourier-Mellin Moments (*QFMM*) of Guo and Zhu (2011) have been rewritten in the Clifford algebra context leading to the definition of the so-called Color Fourier-Mellin Moments (*CFMM*). This rewriting in a more general mathematical framework allows extended choices for a crucial parameter of the method, namely the color analysis plane as defined by two color vectors (a bivector in terms of Clifford Algebras). This parameterization is more natural and easier to handle from an user point of view than the one previously defined in a quaternionic context. Specifically, one can easily discriminate color objects relatively to a prescribed hue. Besides this colorimetric property, a careful examination of the behavior of the moments with respect to usual geometric transforms (translation, rotation, scale) led to the definition of a first set of descriptors. These Color Fourier-Mellin Descriptors (*CFMD*) are shown to be invariant to geometric transformations but are still sensitive to the bivector choice. Depending on the kind of application at hand, e.g. classification or image retrieval, this may be valuable or not. To take into account the cases where no information about such color of interest is available, a bivector insensitive set of descriptor, the *CFMDi*, is also proposed. It must be underlined, that while it does not require the choice of a privileged color plane, it still perfectly discriminates objects of different colors. This is confirmed by experiments on color objects retrieval. When scale change is applied to the considered image data sets, COIL-100 in this article, the *poFMD*, *CFMD* and *CFMDi* outperform Generalized Color Fourier Descriptors (Mennesson et al., 2011), the invariant *poFMD* consistently being the best of the three. Last experiments on image retrieval with scale change unsurprisingly exhibit better results for moment based descriptors and, in such case, we have the following performance ordering : $poFMD > FMM_{rgb} \simeq CFMDi > CFMD > GCFD1$. These results lead to prescribe *poFMD* as a default choice in most cases. From a computational cost perspective, the proposed sets of descriptors depend essentially on the computations of several Fast Fourier Transforms, hence a $O(n\ log(n))$ cost where n is the number of pixels of the considered image.

We have to notice that the choice of a color space (RGB, Lab, XYZ, Ohta, etc.) has been experimented and has shown that it impacts in the similar way the performances of our descriptors and the performance of marginal descriptors. Besides, empirical invariance to every considered transforms and parametrization have been numerically checked. But, due to the lack of space, these results are not shown in this paper.

Finally, as observed in (Andrade et al., 2012; Singh and Sharma, 2013), global and local descriptors can be used together to improve results. Hence, local Color Fourier-Mellin Descriptors extracted in the neighborhood of keypoints (e.g. SIFT (Lowe,

1999)) are under investigations. This, hopefully, will provide robustness against occlusions and non uniform background.

Appendix A. Properties of the *CFMM*

Theorem 1 (Invariance under rotation). *Being a rotation angle ϕ and $f, g \in L^2(\mathbb{R}^2, \mathbb{R}^1_{4,0})$ such as g is a rotated version of f. If we denote $x_1 = rcos(\theta)$ and $x_2 = rsin(\theta)$, then $g(r,\theta) = f(r,\theta+\phi)$ and*

$$CFMM_{g,B}(m,n) = e^{-\frac{n\phi}{2}(B+I_4B)} CFMM_{f,B}(m,n) e^{\frac{n\phi}{2}(B+I_4B)} \tag{A.1}$$

Proof.

$$CFMM_{g,B}(m,n) = \int_{r=0}^{\infty}\int_{\theta=0}^{2\pi} r^{m-1} e^{\frac{n\theta}{2}(B+I_4B)} f(r,\theta+\phi) e^{-\frac{n\theta}{2}(B+I_4B)} d\theta dr \tag{A.2}$$

If we make the substitution $\psi = \theta + \phi$ then

$$CFMM_{g,B}(m,n) = \int_{r=0}^{\infty}\int_{\psi=0}^{2\pi} r^{m-1} e^{\frac{n(\psi-\phi)}{2}(B+I_4B)} g(r,\psi) e^{-\frac{n(\psi-\phi)}{2}(B+I_4B)} d\psi dr \tag{A.3}$$

$$= e^{-\frac{n\phi}{2}(B+I_4B)} CFMM_{f,B}(m,n) e^{\frac{n\phi}{2}(B+I_4B)} \tag{A.4}$$

So, a rotation of the spatial domain implies a phase shift of the Color Fourier-Mellin moments. □

Theorem 2 (Invariance under scale). *Being a scale parameter k and $f, g \in L^2(\mathbb{R}^2, \mathbb{R}^1_{4,0})$ such as g is a scaled version of f expressed in polar coordinates then $g(r,\theta) = f(kr,\theta)$ and*

$$CFMM_{g,B}(m,n) = k^{-m} CFMM_{f,B}(m,n) \tag{A.5}$$

The proof is the same as in (Guo and Zhu, 2011) because a scale change does not affect the CFT *but only the Mellin transform.*

Appendix B. Properties of the *CFMMi*

Theorem 3 (Invariance to bivector B). *Let $f \in L^2(\mathbb{R}^2, \mathbb{R}^3)$, B_1,B_2 two unit bivectors in $\mathbb{R}_{4,0}$ then*

$$CFMMi_{f,B_1}(m,n) = CFMMi_{f,B_2}(m,n). \tag{B.1}$$

Proof. *Let $f(\theta)$ (resp. $\widehat{f_B}(n)$) denotes $f(r,\theta)$ (resp. $\widehat{f_B}(m,n)$) with a fixed r (resp. m). It is obvious that r^{m-1} does not depend on the choice of the bivector, so we only have to prove that*

$$|\widehat{f_B}(n)|^2 + |\widehat{f_B}(-n)|^2 = |\widehat{f_B}(n) + \widehat{f_B}(-n)|^2 + 2\widehat{f_B}(n)\cdot\widehat{f_B}(-n) \tag{B.2}$$

is invariant under the choice of B. Using the generalization of Euler formula for isoclinic 4D rotation

$$\left(\frac{e^{\frac{\theta}{2}(B+I_4B)}\boldsymbol{v}e^{-\frac{\theta}{2}(B+I_4B)} + e^{-\frac{\theta}{2}(B+I_4B)}\boldsymbol{v}e^{\frac{\theta}{2}(B+I_4B)}}{2}\right) = cos(\theta)\boldsymbol{v}, \tag{B.3}$$

the following equation is obtained :

$$\left|\widehat{f_B}(n) + \widehat{f_B}(-n)\right|^2 = \left|\int_{\theta=0}^{2\pi} 2\, cos(n\theta) f(\theta) d\theta\right|^2 \tag{B.4}$$

which does not depend on B. Second term is splitted as $\left(\widehat{f_{\|B}}(n)\cdot\widehat{f_{\|B}}(-n)\right)+\left(\widehat{f_{\perp B}}(n)\cdot\widehat{f_{\perp B}}(-n)\right)$ *where*

$$\widehat{f_{\|B}}(n)\cdot\widehat{f_{\|B}}(-n)=\frac{1}{2}\left(\widehat{f_{\|B}}(n)\widehat{f_{\|B}}(-n)+\widehat{f_{\|B}}(-n)\widehat{f_{\|B}}(n)\right) \tag{B.5}$$

$$=\int_{\theta_1=0}^{2\pi}\int_{\theta_2=0}^{2\pi}f_{\|B}(\theta_1)f_{\|B}(\theta_2)\,cos(n\theta_1+n\theta_2)d\theta_1 d\theta_2 \tag{B.6}$$

Same calculus for $\widehat{f_{\perp B}}(n)\cdot\widehat{f_{\perp B}}(-n)$ *leads to*

$$\widehat{f_{\|B}}(n)\cdot\widehat{f_{\|B}}(-n)+\widehat{f_{\perp B}}(n)\cdot\widehat{f_{\perp B}}(-n)=\int_{\theta_1=0}^{2\pi}\int_{\theta_2=0}^{2\pi}(f(\theta_1)\cdot f(\theta_2))\,cos(n\theta_1+n\theta_2)d\theta_1 d\theta_2 \tag{B.7}$$

We conclude that both terms in Eq. B.2 not depend on B. □

Appendix C. Empirical invariance of descriptors

CFMD	(1, 1)	(2, 1)	(3, 1)	(1, 2)	(2, 2)	(3, 2)	(1, 3)
mean	0.0764	0.0613	0.0172	0.2184	0.3314	0.4167	0.1113
std	0.0004	0.0011	0.0019	0.0020	0.0009	0.0005	0.0009

	$GCFD1_{\|B_{\mathbf{c}}}$			$GCFD1_{\perp B_{\mathbf{c}}}$		
*GCFD*1	1	2	3	1	2	3
mean	3.5 10^6	2.0199	0.7788	1.3 10^6	2.3880	1.2562
std	1.0 10^6	0.0795	0.0209	1.0 10^6	1.0979	2.4273

Figure C.5: *CFMD* and *GCFD1* computed on a non-rotated and non-scaled butterfly image with 100 random bivectors

References

Ahonen, T., Hadid, A., Pietikainen, M., 2006. Face description with local binary patterns: Application to face recognition. Pattern Analysis and Machine Intelligence, IEEE Transactions on 28, 2037–2041.

Andrade, F.S., Almeida, J., Pedrini, H., S.Torres, R., 2012. Fusion of local and global descriptors for content-based image and video retrieval, in: Alvarez, L., Mejail, M., Gomez, L., Jacobo, J. (Eds.), Progress in Pattern Recognition, Image Analysis, Computer Vision, and Applications. Springer Berlin Heidelberg. volume 7441 of *LNCS*, pp. 845–853.

Arbter, K., Snyder, W., Burkhardt, H., Hirzinger, G., 1990. Application of affine-invariant fourier descriptors to recognition of 3-d objects. Pattern Analysis and Machine Intelligence, IEEE Transactions on 12, 640–647.

Batard, T., Berthier, M., Saint-Jean, C., 2010. Clifford fourier transform for color image processing, in: Bayro-Corrochano, E., Scheuermann, G. (Eds.), Geometric Algebra Computing in Engineering and Computer Science. Springer Verlag. chapter 8, pp. 135–161.

Table C.2: The *CFMD*, *CFMDi* and *GCFD1* computed on rotated (R, 35 angles varying from 0° to 350°), scaled (S, 15 scales varying from 0.3 to 1) and rotated+scaled (R+S, 525 angles and scales varying respectively from 0° to 350° and from 0.3 to 1) versions of the butterfly image

$CFMD_{B_{red}}$	Transf.	$(1,1)$	$(2,1)$	$(3,1)$	$(1,2)$	$(2,2)$	$(3,2)$	$(1,3)$
mean	R	0.075	0.060	0.014	0.219	0.332	0.417	0.111
std		0.001	0.001	0.002	0.001	0.001	0.001	0.001
mean	S	0.073	0.061	0.031	0.217	0.331	0.416	0.112
std		0.009	0.010	0.019	0.003	0.002	0.001	0.006
mean	R+S	0.074	0.064	0 .035	0.210	0.328	0.417	0.109
std		0.012	0.015	0.017	0.003	0.002	0.003	0.004

CFMDi	Transf.	$(1,1)$	$(2,1)$	$(3,1)$	$(1,2)$	$(2,2)$	$(3,2)$	$(1,3)$
mean	R	0.037	0.055	0.070	0.055	0.095	0.135	0.035
std ($\times 10^{-4}$)		2	4	5	4	5	6	2
mean	S	0.034	0.051	0.066	0.054	0.094	0.134	0.033
std		0.006	0.007	0.0075	0.002	0.004	0.004	0.003
mean	R+S	0.034	0.051	0.065	0.054	0.093	0.133	0.032
std		0.006	0.007	0.008	0.002	0.003	0.004	0.003

		$GCFD1_{\parallel B_{\mathbf{c}}}$			$GCFD1_{\perp B_{\mathbf{c}}}$		
$GCFD1_{B_{red}}$	Transf.	1	2	3	1	2	3
mean	R	3.3 10^6	2.1987	0.8342	1.6 10^6	1.8748	0.7650
std		3.3 10^4	0.0023	0.0251	1.3 10^4	0.0094	0.0134
mean	S	1.0 10^6	3.9518	3.6761	0.4 10^6	3.7001	3.2325
std		1.0 10^6	1.1496	2.7078	0.5 10^6	1.2270	2.5549
mean	R+S	1.0 10^6	3.9544	3.6593	0.5 10^6	3.7003	3.2247
std		1.0 10^6	1.1113	2.6263	0.5 10^6	1.1889	2.4729

Bornard, G., Gauthier, J.P., Silbermann, M., 1986. Mouvements et traitement d'images. Traitement du Signal 6, 281–290.

Bracewell, R., 1986. The Fourier Transform and Its Applications. McGraw-Hill Companies.

Chang, C.C., Lin, C.J., 2001. Libsvm: a library for support vector machines. Software available at http://www.csie.ntu.edu.tw/ cjlin/libsvm.

Chapelle, O., Haffner, P., Vapnik, V., 1999. Support vector machines for histogram-based image classification. IEEE Transactions on Neural Networks 10, 1055–1064.

Cosgriff, R.L., 1960. Identification of shape. Technical Report ASTIA AD 254-792. Ohio State Univ. Res. Foundation, Columbus.

Derrode, S., Ghorbel, F., 2001. Robust and efficient fourier-mellin transform approximations for gray-level image reconstruction and complete invariant description. Computer Vision and Image Understanding 83, 57–78.

Duda, R.O., Hart, P.E., Stork, D.G., 2001. Pattern Classification. 2nd edition ed., Wiley-Interscience.

Ell, T.A., 1992. Hypercomplex spectral transformations. Ph.D. thesis. Minneapolis, MN, USA.

Ell, T.A., Sangwine, S.J., 2007. Hypercomplex fourier transforms of color images. IEEE Transactions on Image Processing 16, 22–35.

Fenn, M., Kunis, S., Potts, D., 2007. On the computation of the polar fft. Applied and Computational Harmonic Analysis 22, 257 – 263.

Flusser, J., Suk, T., Zitovà, B., 2009. Moments and Moment Invariants in Pattern Recognition. Wiley & Sons Ltd.

Ghorbel, F., 1993. Application de la transformée de fourier généralisée au problème de l'invariance en reconnaissance de formes a niveaux de gris, in: Groupe d'Etudes du Traitement du Signal et des Images (GRETSI), pp. 791–794.

Grace, A.E., Spann, M., 1991. A comparison between fourier-mellin descriptors and moment based features for invariant object recognition using neural networks. Pattern Recognition Letters 12, 635 – 643.

Guo, L.Q., Zhu, M., 2011. Quaternion fourier-mellin moments for color images. Pattern Recognition 44, 187 – 195.

Hestenes, D., Sobczyk, G., 1987. Clifford Algebra to Geometric Calculus : A Unified Language for Mathematics and Physics. volume 5 of *Fundamental Theories of Physics*. Kluwer Academic Publishers, Dordrecht.

Hu, M.K., 1962. Visual pattern recognition by moment invariants. IEEE Transactions on Information Theory 8, 179–187.

Jain, A.K., Murty, M.N., Flynn, P.J., 1999. Data clustering: A review. ACM Comput. Surv. 31, 264–323.

Liu, H., Guo, B., Feng, Z., 2006. Pseudo-log-polar fourier transform for image registration. Signal Processing Letters, IEEE 13, 17–20.

Lowe, D.G., 1999. Object recognition from local scale-invariant features, in: ICCV, pp. 1150–1157.

Mennesson, J., Saint-Jean, C., Mascarilla, L., 2010. New geometric fourier descriptors for color image recognition, in: Image Processing (ICIP), 2010 17th IEEE International Conference on, pp. 2685 –2688.

Mennesson, J., Saint-Jean, C., Mascarilla, L., 2011. Color object recognition based on a clifford fourier transform, in: Dorst, L., Lasenby, J. (Eds.), Guide to Geometric Algebra in Practice. Springer London, pp. 175–191.

Mennesson, J., Saint-Jean, C., Mascarilla, L., 2012. Un nouvel ensemble de descripteurs de Fourier Clifford pour les images couleur : les GCFD3. Traitement du Signal 29, 359–382.

Mikolajczyk, K., Schmid, C., 2005. A performance evaluation of local descriptors. IEEE PAMI 27, 1615–1630.

Nene, S.A., Nayar, S.K., Murase, H., 1996. Columbia object image library (coil-100). Technical Report CUCS-006-96.

Phillips, P.J., Wechsler, H., Huang, J., Rauss, P., 1998. The feret database and evaluation procedure for face recognition algorithms. Image and Vision Computing 16, 295–306.

Rosten, E., Porter, R., Drummond, T., 2010. Faster and better: A machine learning approach to corner detection. IEEE PAMI 32, 105–119.

Sangwine, S.J., Ell, T.A., 2000. The discrete fourier transform of a colour image, in: Blackledge, J.M., Turner, M.J. (Eds.), Image Processing II: Mathematical Methods, Algorithms and Applications, Horwood Publishing for Institute of Mathematics and its Applications. pp. 430–441.

Sheng, Y., Arsenault, H.H., 1986. Experiments on pattern recognition using invariant fourier-mellin descriptors. The Journal of the Optical Society of America A 3, 771–776.

Singh, C., Sharma, P., 2013. Performance analysis of various local and global shape descriptors for image retrieval. Multimedia Systems 19, 339–357.

Smach, F., Lemaître, C., Gauthier, J.P., Mitéran, J., Atri, M., 2008. Generalized fourier descriptors with applications to objects recognition in svm context. Journal of Mathematical Imaging and Vision 30, 43–71.

Teague, M.R., 1980. Image analysis via the general theory of moments. Journal of the Optical Society of America (1917-1983) 70, 920–930.

Vapnik, V.N., 1998. Statistical Learning Theory. Wiley-Interscience.

Zernike, v.F., 1934. Beugungstheorie des schneidenver-fahrens und seiner verbesserten form, der phasenkontrastmethode. Physica 1, 689 – 704.

Zhang, D., Lu, G., 2002. Shape-based image retrieval using generic fourier descriptor. Signal Processing: Image Communication 17, 825 – 848.